Proceedings of ICRC 2001: 543 © Copernicus Gesellschaft 2001

ICRC 2001

Size of optical image of an air shower

D. Góra, P. Homola, M. Kutschera, J. Niemiec, B. Wilczyńska, and H. Wilczyński

Institute of Nuclear Physics, Kraków, Poland

Abstract. Distribution of photons which form a shower image is simulated. Using a realistic distribution of particles in the shower, and taking atmospheric scattering of light into account, one obtains a distribution of photons which were emitted at the shower front and arrive simultaneously to the eye. These photons form an instantaneous image of the shower, although they originate from a range of shower development stages. The angular size of this image is studied and compared with a detector pixel size.

1 Introduction

Extensive air showers can be detected by recording fluorescence light emitted by air molecules which get excited by charged particles of the shower. Since the photon yield is approximately constant per unit length of a charged particle trajectory in the air, the amount of fluorescence light is a direct measure of the number of particles in the shower. A large number of charged particles in a high energy shower (10^{10} particles in maximum shower development) produces enough fluorescence light so that the showers can be detected from a distance of many kilometers by an appropriate optical instrument. This technique was first used in the Fly's Eye experiment (Baltrusaitis, 1985).

Secondary particles in a shower front form a disk perpendicular to the shower axis. Most of these particles are collimated near the shower axis, within distances on the order of the Molière radius ($\sim$ 80 m at sea level). Thus, when seen from a large distance, the shower resembles a luminous point moving with a speed of light, as if all particles of the shower were grouped at the shower axis. For showers near the detector, however, the shape of lateral distribution of shower particles is important.

The shape of shower image was studied in (Sommers, 1995) and shown to be of circular shape, even when the shower is viewed perpendicularly to its axis. In this paper, we show a detailed simulation of the shower image, using a realistic particle distribution in the shower front and taking into account light scattering in the atmosphere.

Correspondence to: H. Wilczyński
(Henryk.Wilczynski@ifj.edu.pl)

2 Details of shower image

When a circular shower front moves with a speed of light, photons which were emitted simultaneously at the shower front do not necessarily arrive simultaneously at the eye. Conversely, the photons which constitute the shower image (i.e. which arrive simultaneously to the eye) must have originated at different times from different shower development stages. This situation is illustrated in Figure 1. In this Figure, a disk-like shower front with radius R is sketched, moving along the shower axis $\boldsymbol{u}$. Let us consider the shower front when it is at position marked **m** in Fig. 1. Photons emitted simultaneously from points A and B do not arrive simultaneously at the eye since the distances of these points from the eye are clearly different (labelled d_i and L respectively). By the time a photon emitted at B arrives to an intermediate point D in the vicinity of point A, the shower front moves downstream to a new position marked **n** in Figure 1, such that distance BD=AC=δ_i. Since distances OD=OC, a photon emitted at point C, rather than A, will arrive to the eye simultaneously with a photon from B. In other words, simultaneous arrival from points B and C requires that the time of speed-of-light travel from B to O be the same as from A to C plus C to O, i.e. $L = \delta_i + CO$. Thus, we get

$$\delta_i = \frac{L^2 - d_i^2}{2(L - d_i \cos\theta_i)} \tag{1}$$

where θ_i is the angle between the shower axis and the direction towards the eye. This formula can be applied to each point of shower front **m** to find the corresponding displacement δ_i. Hence, the photons arriving simultaneously to the eye originate from a surface S similar to the shaded one in Figure 1, and not from a single stage of shower development.

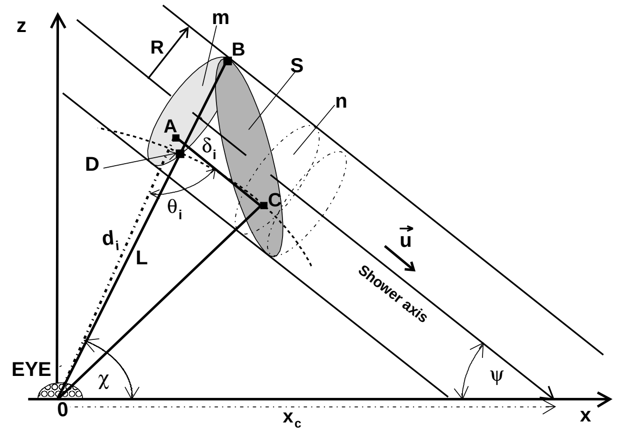

Fig. 1. Geometry of an extensive air shower as seen by the fluorescence detector. The shower front of radius R moves through the atmosphere in direction $\boldsymbol{u}$. Photons which arrive simultaneously to the eye (i.e. those which constitute the shower image) originate from surface S. See text for more details.

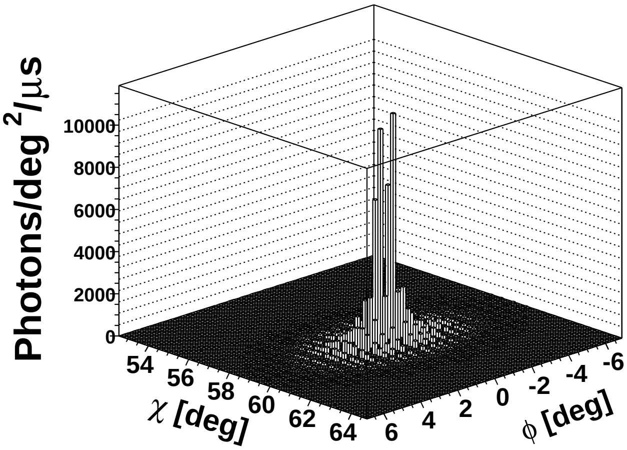

Fig. 2. An example of a snapshot image of a shower: distribution of light on the sky in elevation angle χ and azimuth ϕ.

The lateral distribution of particles in the shower front is parameterized by the Nishimura-Kamata-Greisen (NKG) function

$$\rho(r) = \frac{N(X)}{r_M^2}(\frac{r}{r_M})^{s-2}(1+\frac{r}{r_M})^{(s-4.5)}\frac{\Gamma(4.5-s)}{2\pi\Gamma(s)\Gamma(4.5-2s)} \quad (2)$$

with the total number of particles $N(X)$ given by the Gaisser-Hillas function

$$N(X) = N_{max}(\frac{X-X_0}{X_{max}-X_0})^{(X_{max}-X_0)/\lambda}\exp^{((X_{max}-X)/\lambda)} \quad (3)$$

N_{max} is the number of particles at maximum shower development, where X is the slant atmospheric depth, X_0 – depth of first interaction, X_{max} – depth of maximum shower development, λ – interaction length in the air (70 g/cm^2), s – shower age parameter ($s = 1$ at shower maximum) and r_M – the Molière radius. The Molière radius determines the lateral spread of particles in the shower due to multiple scattering in the air. Since the temperature and pressure change along the shower path, so does the Molière unit.

The distribution of particles in a shower at a given depth depends on the history of r_M changes along the shower path more than on the local r_M value at this depth. To take this into account one uses the r_M value calculated at 2 cascade units above the current depth (Greisen, 1956; Matthews, 1998):

$$r_M[metres] = 272.5\frac{T[K](\frac{P[mb]-73.94\cos\theta}{P[mb]})^{1./5.25588}}{P[mb]-73.94\cos\theta} \quad (4)$$

A real shower front is not a flat disk. It can be approximated by a spherical surface with curvature $R_c = 9000\sec(\vartheta) - 3600$ meters (typically $\sim$ 10 km), where ϑ is the shower zenith angle. Thus one can completely parameterize the particle distribution in the shower, including variations of both longitudinal and transverse distributions over the surface S from which the simultaneous photons originate (see Figure 1).

The shower particles generate a large number of Čerenkov photons in the air. Contrary to fluorescence photons, which are emitted isotropically, the Čerenkov photons are beamed primarily along the shower axis. These photons undergo scattering in the atmosphere by Rayleigh process (scattering on molecules of air) and Mie scattering (on aerosols), and some of them may reach the eye. In consequence, the light received by the detector eye is composed not only of fluorescence photons, but has an admixture of scattered Čerenkov photons – and in some cases even "direct" Čerenkov photons can reach the eye. In the following, we show results on showers in which Čerenkov photons make only a small contribution (less than 20 %) to the light received.

Technically, the distribution of photons over the surface S from which simultaneous photons originate, is obtained first. Next, these photons are propagated towards the eye, taking into account light scattering in the air. Finally, the angular distribution of these photons arriving simultaneously is constructed to form the image of the shower. An example of light distribution in the shower image is shown in Figure 2. More details on the simulation procedure are given in an upcoming paper (Góra et al., 2001). We stress that we discuss here the light *arriving* at the eye; no detector properties are discussed.

3 Image size

Simulation runs were done using the `Hybrid_fadc` simulation software (Dawson, 1998) for showers at fixed energy $E = 10^{20}$ eV and depth of first interaction at $X_0 = 70$ gcm^{-2}, and with variable core distance x_c (see Fig. 1) and shower inclination angle ψ. Showers landing at $x_c = 3$ km, 7 km and 15 km were studied at inclination angles ψ varying from 30° to 150°. The details of shower image analysis can be found in (Góra et al., 2001); here we will only comment on the final result.

Depending on the core distance and inclination angle, the showers reach their maxima at various distances from the

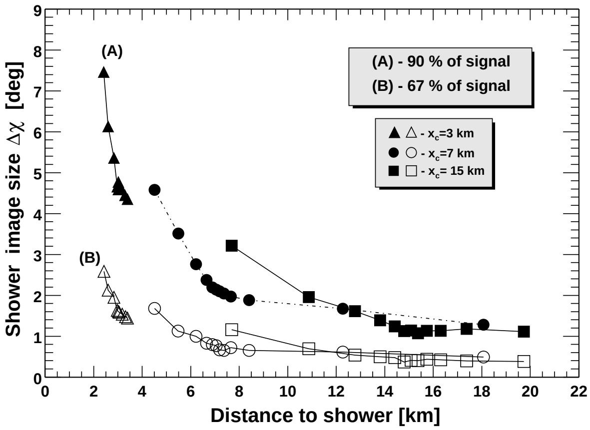

Fig. 3. Size of the shower image containing 90% of the light versus distance to the shower, for showers landing at 3, 7 and 15 km from eye. The spot sizes corresponding to 90% of the signal (A) and 67% (B) are shown.

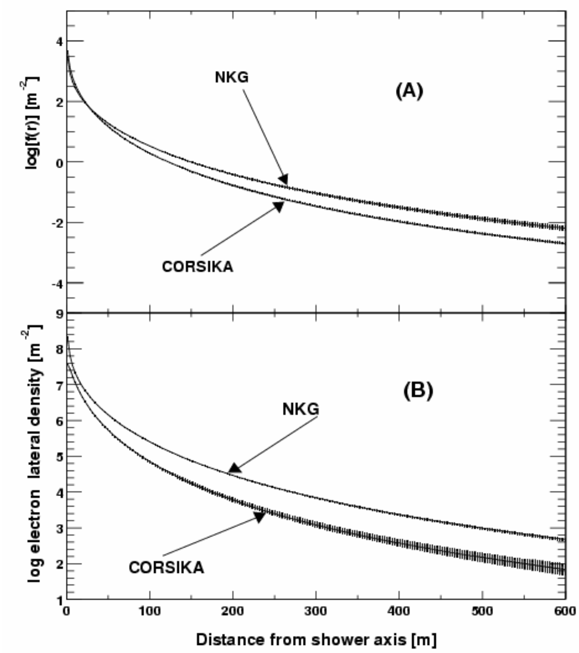

Fig. 4. Shapes of lateral distribution function $f(r)$ in CORSIKA and NKG are shown in panel (A); the lateral densities are shown in panel (B).

eye. Their images at the eye must obviously have different angular sizes. Moreover, the inclined showers encounter more air along their path so that they reach their maxima higher above the ground than showers incoming vertically. The density of air at higher elevation is smaller, so in consequence the Molière radius is larger. Since the Molière radius determines the lateral spread of particles in a shower, the inclined showers are inherently wider than vertical ones and so their images in the detector must be larger.

The image spot size containing 90% of light is plotted in Figure 3 as a function of distance to the shower, for showers with different ψ and x_c. The 'distance to shower' is the distance from the eye to a point on the shower axis from which maximum signal is received. The simulated data points for showers with the same core distance, but different inclination angles, follow a V-shaped curve, which reflects the changes of the Molière radius with altitude. The 90% spot size is larger than 1.5 degrees pixel size for nearly all showers studied. However, restricting the image to its brightest part containing 67% of the signal, results in much smaller image size which is below 1° for most of showers (points marked B on Fig. 3).

The results presented above were obtained for "generic" showers as given by the NKG and Gaisser-Hillas functions, used in the `Hybrid_fadc` program. These functions describe average showers of a given energy and are insensitive to mass of primary particle which initiated the shower. In order to simulate the showers more precisely, the CORSIKA 6.00 simulation program was used with QGSJET nuclear interaction model. In this software, individual showers are simulated, including distributions of particles produced in the many individual interactions. All particles are propagated through the air, with an appropriate thinning algorithm, and simulating the subsequent interactions. At any depth in the atmosphere, the total number of particles in the shower is obtained together with their lateral distribution around the shower axis. As a result, not only more realistic particle distributions are produced, but also shower-to-shower fluctuations are reproduced. Averaging over many showers is then necessary to get the "average" shower of interest.

A comparison of lateral distributions of shower particles in CORSIKA and that given by NKG function was made. Since the lateral distribution $\rho(r) = N(X) \cdot f(r)$, one can compare separately the longitudinal shower development $N(X)$ and the lateral shape function $f(r)$. The number of particles at shower maximum, as given by CORSIKA and `Hybrid_fadc` differ considerably: CORSIKA produces about 20% less particles. The lateral shape functions $f(r)$ are compared in Figure 4(A). In panel (B) of this figure a comparison of full densities $\rho(r)$ is shown. It is seen that the CORSIKA distribution is narrower. An immediate consequence is that the shower image simulated using CORSIKA lateral distribution should be somewhat smaller than that shown in Figure 3. Indeed, the preliminary result is that the spot sizes analogous to those in Fig.3 are about 25% smaller when CORSIKA is used for shower simulation. This demonstrates the importance of accuracy of shower simulation. Further work is in progress.

Finally, a comparison of lateral distributions of proton-induced and iron-induced showers is shown in Figure 5. Figure 5(A) shows the lateral shape function $f(r)$ for proton and iron showers at atmospheric depth 650 g/cm^2 (i.e. before both shower maxima), and Fig. 5(B) – at depth 1050 g/cm^2 (after both maxima). No difference between proton and iron showers can be seen. This means that the lateral distribution of particles in a shower is determined by multiple scattering in the air much more than by kinematics of the

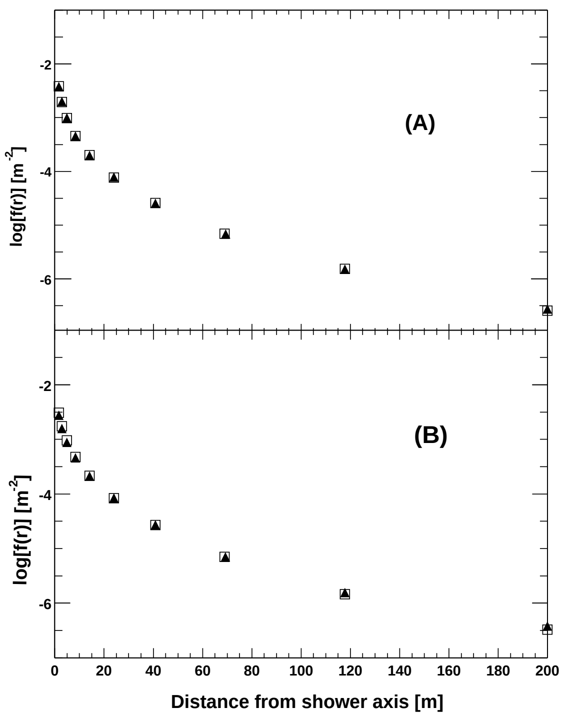

Fig. 5. Comparison of lateral shape function in proton-induced showers (open squares) and in iron-induced showers (black triangles) in CORSIKA. Panel (A) shows the distribution at depth 650 g/cm^2, and panel (B) – at 1050 g/cm^2.

primary interaction.

4 Conclusion

Since the shower front moves with the speed of light, the optical image of a shower is always composed of photons emitted from a range of shower development stages. In consequence, one never actually sees the shower front edge-on, irrespectively of the shower geometry. The image of a shower is a spot of light with intensity strongly peaked at its center. The light distribution resembles the NKG lateral distribution of particles in the shower front.

The size of the image spot depends not only on the distance to the eye, but also on the Molière radius, which determines the lateral spread of particles in the shower. Inclined showers generally develop higher in the atmosphere and so their images are larger. The image spot containing 90% of the light has a diameter larger than 1 degree for most showers. With decreasing distance the spot size increases and reaches about $4°$ for showers at a distance of 5 km. The variation of the size due to to varying Molière radius is about 1 degree. This implies that in a detector with $1.5°$ pixel size, like the Pierre Auger Project fluorescence detector, the shower image will often cover more than a single pixel. Thus adding signals from several pixels will be necessary for precise energy measurement with the fluorescence detector. Although the full shower image is wide, its central brightest part is much smaller. The spot size containing 67% of the signal is smaller than $1°$ for showers at 5 km distance, and about $0.5°$ for those at distance ~ 20 km. The center of the image is therefore well defined, so that geometry of the shower can be satisfactorily reconstructed.

The size of shower image does not depend on primary particle which initiated the shower, but is determined by multiple scattering of shower particles in the air.

Acknowledgements. This work was partially supported by the Polish State Committee for Scientific Research under grant No. 2 P03B 112 17.

References

Baltrusaitis, R.M. et al., Nucl. Instr. Meth. A240, 410-428 (1985).
Dawson, b., private communication (1998).
Góra, D et al., Astropart. Phys., in print (2001).
Greisen, K., Prog. in Cosmic Ray Phys. 3, 1 (1956).
Matthews, J.A.J., Pierre Auger Project Note: GAP-98-002 (1998).
Sommers, P., Astropart. Phys. 3, 349-360 (1995).